Metallurgical and Materials Data 3, no. 2 (2025): 53-64

Publisher: Association of Metallurgical Engineers of Serbia

Metallurgical and Materials Data

www.metall-mater-data.com

Fabrication and characterization of tungsten-based hard materials by novel mechanical alloying and spark plasma sintering methods

Muddassar Hussain*[,1,2], Muhammad Zarif[3], Ha iz Zahid Sha i[4], Fasial Shahzad[5], Maria Gul[6], Muhammad Hassan[7], Abbas Saeed Hakeem[8], Zafar Iqbal[3]

[1]*Pakistan Institute of Nuclear Science and Technology (PINSTECH), Islamabad, Pakistan*
[2]*Pakistan Institute of Engineering and Applied Sciences (PIEAS), Department of Nuclear Engineering, Nilore, Islamabad, Pakistan*
[3]*Pakistan Institute of Engineering and Applied Sciences (PIEAS), Department of Metallurgy and Materials Engineering, Islamabad, Pakistan*
[4]*National Institute of Lasers and Optronics, Islamabad, Pakistan*
[5]*Khalifa University, Abu Dhabi, United Arab Emirates*
[6]*Pakistan Institute of Nuclear Science and Technology (PINSTECH), Physics Division, Islamabad, Pakistan*
[7]*National Centre for Physics, Islamabad, Pakistan*
[8]*King Fahd University of Petroleum and Minerals Interdisciplinary Research Center for Hydrogen & Energy Storage (IRC-HES)*

ARTICLE INFORMATION:

https://doi.org/10.56801/MMD53

Received: 21 April 2025
Accepted: 12 May 2025

Type of paper: Research paper

ABSTRACT

The influence of Ir and Y_2O_3 on the densification, microstructure, and wear characteristics of pure W-based alloy/composite was examined. The precursor powders, including W, Ir, and Y_2O_3, underwent mechanical alloying for 30 hours, resulting in two compositions: W–1.5 wt.% Ir and W–1.5 wt.% Ir–2 wt.% Y_2O_3. Subsequently, the prepared mixtures were subjected to spark plasma sintering at a temperature of 1650 °C for 5 minutes, with a simultaneous application of 50 MPa pressure. X-ray diffraction, scanning electron microscopy combined with energy dispersive spectroscopy, a micro-Vickers hardness tester, and two-dimensional optical profilometry were employed to analyze the synthesized powders, along with the consolidated and worn samples. Results indicated that the W–1.5 wt. % Ir-2 wt. % Y_2O_3 composite produced a highly dense sample characterized by the smallest grain size, superior micro-hardness, and enhanced wear resistance. The composite achieved values of up to 98% density, 3.6 µm grain size, 4.9 GPa $HV_{0.5}$ hardness, and 2.5×10^{-5} mm^3/Nm wear resistance, in contrast to pure tungsten, which exhibited 83.1% density, 6.6 µm grain size, 1.9 GPa $HV_{0.5}$ hardness, and 6.2×10^{-5} mm^3/Nm wear resistance. Thus, both Ir and Y_2O_3 have been recognized as effective additives that can enhance the consolidation and refinement of tungsten's microstructure under current mild processing conditions. This advancement not only makes these materials commercially viable but also enhances their performance in a range of demanding applications, such as fusion, military, tooling, electrode manufacturing, and coatings.

Keywords: mechanical alloying, spark plasma sintering, tungsten-iridium-yttria composite, consolidation behavior, microstructure, wear and tribology.

1. Introduction

Tungsten (W) possessed outstanding characteristics such as high density, high hardness, high melting point, minimal sputtering yield, superior thermal conductivity, and a low thermal expansion coefficient(Pitts et al. 2013; Chen and Sutrisna 2022). This makes tungsten a promising candidate for high-temperature and wear resistant applications such as, plasma-facing materials in fusion energy technologies, radiation shielding in the nuclear industry, kinetic energy penetrators in military, and wear-resistant coatings for space automotive industry, pin tool material in friction stir welding process, electrode in welding and melting processes etc.9(Lau et al. 2023; Riesch et al. 2024; Oshrieh et al. 2024; Mishra and Ma 2005; Rahul et al., n.d.; Wahid et al. 2016; Rai et al. 2011; Chiteka 2013; Iqbal, Saheb, and Rahman 2016; Thompson 2011). The key drawbacks associated for its commercial viability and effective utility are high melting point, high ductile-brittle transition temperature (DBTT)(Yin et al. 2021), high temperature brittleness due to recrystallization as well as radiation(Yin et al. 2020; H. W. Deng et al. 2018). Fine-grained W materials have shown attractive properties in terms of reduction in brittleness and improvement in toughness and strength (Shah et al. 2020).

Fabrication techniques influence the densification, microstructures and all related properties of the sintered metals(Debata, M., Sengupta, P., Mandal, S., Adhikari, n.d.; Barua et al. 2024; Saheb et al. 2012; G. Lee et al. 2016; S. Deng et al. 2017; Ayodele et al. 2018; Nisar et al. 2021; Muñoz et al. 2014; Yar et al. 2011; Alloys 2016; Froes et al. 1998;

* Corresponding author.
E-mail address: muddassarhussain505@gmail.com (Muddassar Hussain).

Pramanik et al. 2019).Similarly; addition of suitable alloying elements/ reinforcements to tungsten not only impart useful properties but also eases the fabrication of these materials(X. Li et al. 2022; Lang et al. 2025; T. Li et al. 2023; Chanthapan et al. 2012; Nygren et al. 2011; Ren et al. 2016; Oda, Ameyama, and Yamaguchi 2006; Fan et al. 2014; Dong et al. 2017; M. Wu et al. 2021).

Hot isotactic pressing of pure tungsten powder at 20000C and 85 MPa for 5 minutes resulted in a relative density of 97% and a mean grain size of 10.6 μm, respectively (Chanthapan et al. 2012). The addition of low-cost transition metal such as Ni, Fe, Co, Mo, and V can greatly enhance the sinterability of tungsten but also degrade its high temperature properties. As Ni, Fe, Co provide liquid phase during sintering which enhances consolidation but lead high grain growth and result to degrade the mechanical properties(Zhang et al. 2009). Similarly, the Mo and V may result in degradation high temperature strength or stability of structural member because of reduction in elastic moduli with temperature. Study revealed that the Vanadium and Molybdenum has Elastic Modulus of 128 GPa and 329 GPa at room temperature respectively(Snead et al. 2019).The low oxidation resistance of Mo also restricted its widespread use for high temperature application(Parthasarathy, Mendiratta, and Dimiduk 2002)

Alternatively, platinum group metals such as Re, Ir, Os, and Rh have shown excellent characteristics when alloyed with tungsten(Karafi et al. 2023; Siller et al. 2023; Que et al. 2025; Yamamoto, Hara, and Hatano 2021) They enhanced the sinterability by acting as a solid-state sintering activator instead of a liquid phase, refines grain structure, increases grain boundaries cohesion, cleanses grain boundaries by reacting with impurities (Verma et al. 2025; Lakshmi Prasad and Raja Annamalai 2021; Samsonov and Yakovlev 1970; Hayden and Brophy 1963; Bose, Sadangi, and German 2012; Blagoveshchenskiy et al. 2018; Setyawan and Kurtz 2012; Kiran et al. 2017; M. Zhao et al. 2015; German 2015; R.M .GERMAN 1977; Shabalin 2019; Watanabe et al. 2019; Yujin Wang et al. 2011)].Iridium showed the highest Young's Modulus of all face-centered cubic metals and the highest modulus of rigidity of all metals. At 1000°C the Modulus of Rigidity was still 170 GPa and Young's Modulus 417 GPa.Young's Modulus could be measured up to 1300°C (382 GPa)(Merker et al. 2001). Iridium addition also showed excellent high temperature oxidation resistance.

Similarly; Researchers examined how the hard particles such as ZrC, Y2O3, La2O3, and HfO2 affected the sintering behavior of W and discovered that they improved the densification of W compacts while maintaining a small grain size[(Heo et al. 2022; Marchhart et al. 2024;(Veleva et al. 2009; Liu et al. 2018; Yiming Wang and Aktaa 2017; Liu et al. 2016; D. Lee et al. 2014; J. Lee et al., n.d.; German, Meyer, and Ei-desouky 2012; Liu et al. 2014; E. S. Lee et al. 2022; S. Zhao et al. 2024; L. Li et al. 2023).

Under mild processing conditions, it is challenging to fabricate dense and fine-grained tungsten-based materials because increasing the temperature, pressure, and time to achieve fully dense tungsten results in large grain structure, which makes it economically unfeasible and leads to poor microstructural characteristics and, ultimately, performance. This research work attempts to address this issue by altering the composition, for example, by adding iridium and yttrium oxide particles. The results showed that adding both iridium and yttria to the tungsten produced nearly fully densely with relatively fine-grained tungsten-based material as compared to pure tungsten under the same processing conditions. This makes tungsten-based materials more economically viable as well as improving their performance in a range of engineering applications. The primary goal of the current study was to produce fine-grained and dense tungsten-based materials. The tribological performance of developed material's was thoroughly examined for wear resistant applications, such as tooling.

2. Experimental procedures

The W-1.5wt. %Ir-2Y_2O_3 composite material was synthesized in two stages. In first stage ,W and Ir powders of purity >99.9% from BDH, UK, and sigma Aldrich, Germany with an average particle sizes of 1.8 μm, 0.6, were mechanically alloyed with W 1.5wt.% Ir combination in a high energy planetary ball mill (Fritsch Pulverisette P-6, Germany) at a speed of 250 rpm with a ball to powder weight ratio of 8:1 for 20h. The balls of 10 mm diameter and vials are made up WC material. Once an alloy of was prepared after 20 hours, in the second stage the Y_2O_3 particles of purity >99.95 wt.% with an average particle size 2 μm from sigma Aldrich, were added to W 1.5wt.% Ir alloy prepared during first stage and further in-situ milled for 10 hour to disperse homogeneously within alloy matrix. Total milling time is kept 30 hours for both alloy and composite powders Powder samples were taken after an interval of 10 hours. Then, as prepared powders were introduced in a 20 mm diameter graphite cylindrical die with a vacuum level of 10^{-3} mbar in spark plasma sintering (FCT system HP D5, Germany). The conditions for sintering kept same for all materials as follows (T= 1650°C, P =50 MPa, and t= 5min.). The temperature of the die was gradually raised to 1650°C and held constant at this temperature for 5 minutes. The heating rate of 100°C/min and a constant pressure of 50 MPa maintained throughout the spark plasma sintering (SPS) cycles. For comparison, pure tungsten was milled and subsequently sintered under same conditions.

The microstructure of powder particles and of sintered bodies was studied using scanning electron microscopy/energy dispersive spectroscopy (SEM/EDS) as well as X-ray diffraction (XRD) measurements to get in depth insight about presence and distribution of phases, formation of alloy and composite, and particle and crystallite sizes. The parameters utilized for the XRD analysis included a starting angle of 10 degrees, a stopping angle of 90degrees, a step size of 0.02 degrees, and copper (Kα: 0.154 nm) served as the radiation source. The Crystallite sizes were calculated using single line Voigt method (Basak, Nath, and Das 2023). Dislocation density (ρ) was estimated using the formula in equation $\rho = \frac{2\sqrt{3}\left(\varepsilon_0^{\,2}\right)^{0.5}}{db}$, where b is magnitude of Berger's vector for dislocation, for bcc tungsten it is equal to $\frac{a\sqrt{3}}{2}$, d is crystallite size in nm , a is lattice parameter in nm, and root mean strain($\left(\varepsilon_0^{\,2}\right)^{0.5}$) is equal to $\varepsilon\frac{2}{\pi}$, ε is normal strain (Vaneela 2017).

The average grain/particles sizes were estimated by conventional metallographic methods using Image J software. The metallographic preparation of sintered compacts involved grinding unto SiC emery paper (No. 3000) and then polished to a mirror finish using 0.3 μm suspended alumina (Al2O3) slurry. After grinding and polishing, electrolytic etching was performed in 0.1M solution of NaOH at 5V for 5-10 seconds. The densities of the consolidated samples were measured by Archimedes' principle(EN ISO 3369 2010). The relative densities were calculated by simply taking ratio of Archimedes to theoretical density. The theoretical densities for 1.5wt% Ir and 2wt% Y2O3 reinforced samples were calculated using rule of mixture as follows $\frac{1}{\rho_m} = \sum_{i=1}^{n} \frac{wi}{\rho i}$ where ρm is the density of mixture(alloy/composite)wi mass fraction and ρi is the theoretical density of given components(e.g. i=1,2,3....n) in the mixture. The theoretical densities of constituent elements in their pure form are given as W (19.34 g/cm³), Ir (22.40 g/cm3), and Y2O3 (5.01 g/cm³) respectively(Dong et al. 2019). For comparison, pure tungsten was also milled as well as sintered at same processing conditions.

Micro hardness of sintered specimens was determined using a Vickers micro hardness tester (LECO Instrument GmbH) by applying 0.5 kg load for 15 sec and 10 measurements were taken for each

sample then averaged out these values to get Vickers hardness number (VHN). Wear tests were carried out with pin-on-disc sliding setup at relative humidity of 50% and at room temperature (25 °C, RT), using Nanovea Pin on Disk Tribometer Model MT/60/NI. A capacitive sensor and software equipped with MFT5000 apparatus was attached with tribometer was used to measure the wear rate, coefficient of friction. Whereas, the specific wear rate, expressed in mm^3/Nm, was calculated by dividing measured wear rate with sliding distance. The counter pin of hardened alloy steel was chosen to induce wear to study the wear performance and behavior. Tribological test against 6 mm steel pin was performed at a constant 30N normal load and RT with relative humidity of 50%. The sliding distance and speed was maintained at 30m and 100 rev/min respectively, for all the sliding tests. The wear tracks were characterized using SEM and EDS analysis to observe the wear mechanism. The surface topography of wear tracks was measured using 2D optical profilometry (PS-50, NANOVEA, USA) which projects light onto the surface and captures the reflected light, creating a 2D image of the surface profile. This surface roughness profile contained various parameters that can be used to quantify the wear occurred in materials.

3. Results and Discussion

Figure 1a- c illustrate the morphology of as received powders. Both tungsten and iridium powders exhibit cuboid shapes and smooth surfaces, while the yttrium oxide powder is characterized by its flaky nature. The particle size distribution for the initial tungsten, iridium, and yttria powders follows a Gaussian distribution, with average particle sizes (Davg) of 1.8 µm, 0.6 µm, and 2.0 µm, respectively.

FE-SEM micrographs of the pure tungsten (W), the W-1.5 wt.% iridium (Ir) alloy, and the W-1.5 wt. % Ir-2Y2O3 composite powder particles following 30 hours of ball milling presented in Figure 2a-c. The pure tungsten displays a flat morphology, while both the alloy and composite reveal a spherical morphology in their powder particles. Additionally, the presence of particle agglomeration in the composites suggests the extremely fine characteristics of the powder particles. The composite exhibits the smallest average particle size (Davg = 53±2 nm), which is smaller than that of the alloy (Davg = 59±0.1 nm) and pure tungsten (Davg = 89±4.2 nm). This reduction in particle size can be attributed to the presence of hard yttria particles that function as milling media, facilitating the size reduction process. Consequently, the atoms of tungsten, iridium, and yttria intermingle and achieve a more uniform distribution within the powder, resulting in a homogeneous composite powder, as illustrated in Figure 3 below.

Similarly, the XRD analysis of as received, mixed and milled (mechanically alloyed) tungsten iridium alloy and tungsten-iridium-yttria composite powders can be seen in Figure 4. The diffraction patterns of as received tungsten and iridium powders show reflection peaks correspond to cubic phase with space groups of cubic: Im-3m and cubic: Fm-3m, while and yttria powder shows reflection peaks which corresponds to cubic: Ia-3 phase, respectively. Iridium and yttria are present in trace amounts, so peaks related to iridium and yttria are not observed in X-ray diffraction (XRD) patterns of milled alloy and composite powders, However, their presence is evidenced by EDX analysis (Figure 3).

It can be noticed in Figure 4 that all the reflection peaks in case of tungsten-iridium blend shifted continuously towards higher angles after 10 hours of milling and up to 30 hours. This peak shifting is due to alloying of iridium in tungsten lattice. As Iridium possesses a smaller atomic radius of 180 pm, while tungsten has an atomic radius of 193 pm. Consequently, when iridium is substituted for tungsten, the lattice parameter or interplanar spacing of tungsten decreases, leading to a shift of the peak towards a higher angle, as described by Bragg's law ($n\lambda=2d\sin\theta$). Thus, it implies that milling leads to formation of single-phase bcc solid solution of W-1.5 wt.% Ir alloy.

The asymmetric change in peak shape for W-1.5 wt.% Ir showed the introduction of non-uniform strains/dislocations in tungsten lattice that may cause to refine the grain size (Table 1). Similarly, for W-1.5wt. %Ir-2Y_2O_3 composite all peaks except the first intense peak seems to be vanished (show negligible intensity), and shift toward lower angle. it may attribute to dissolution of large yttrium atom having atomic radius of 212pm as detected by energy dispersive x-rays (EDX) and elemental mapping analysis in Figure 3. Moreover, milling also leads to peak broadening. The occurrence of X-ray diffraction peak broadening is associated with defect accumulation (strains) and crystallite size reduction (Table 1). In Table 1 it can be seen that smallest crystallite size is obtained in case of composite and alloy than pure tungsten. This could be the result of the iridium atom being added, which modifies the tungsten's dislocation core structure similarly to Re. It also brings a complex dislocation mechanism to tungsten, which tends to accelerate the formation and multiplication of dislocations and causes new, smaller grains to rearrange (Karafi et al. 2023). Likewise, in composite materials, the elevated dislocation density attributed to the hard yttria particles which lead to a further diminishment of crystallite size.

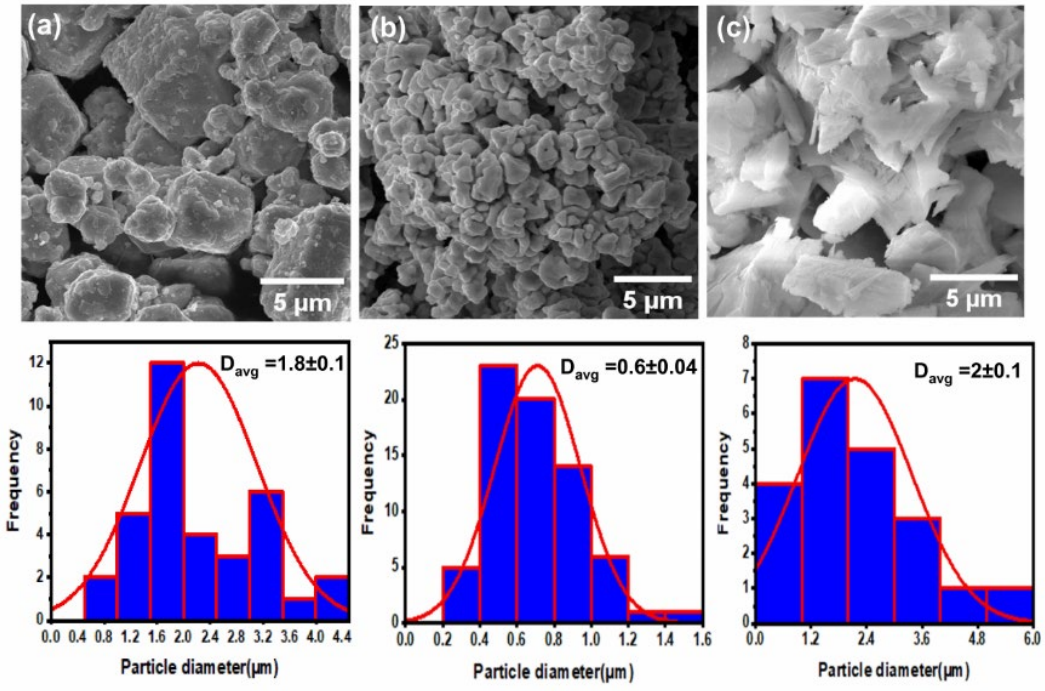

Fig. 1. FE-SEM-Secondary micrograph, particle size distribution, and average particle size (D_{avg}) of initial (a) W, (b) Ir, and (c) Y_2O_3 starting powders.

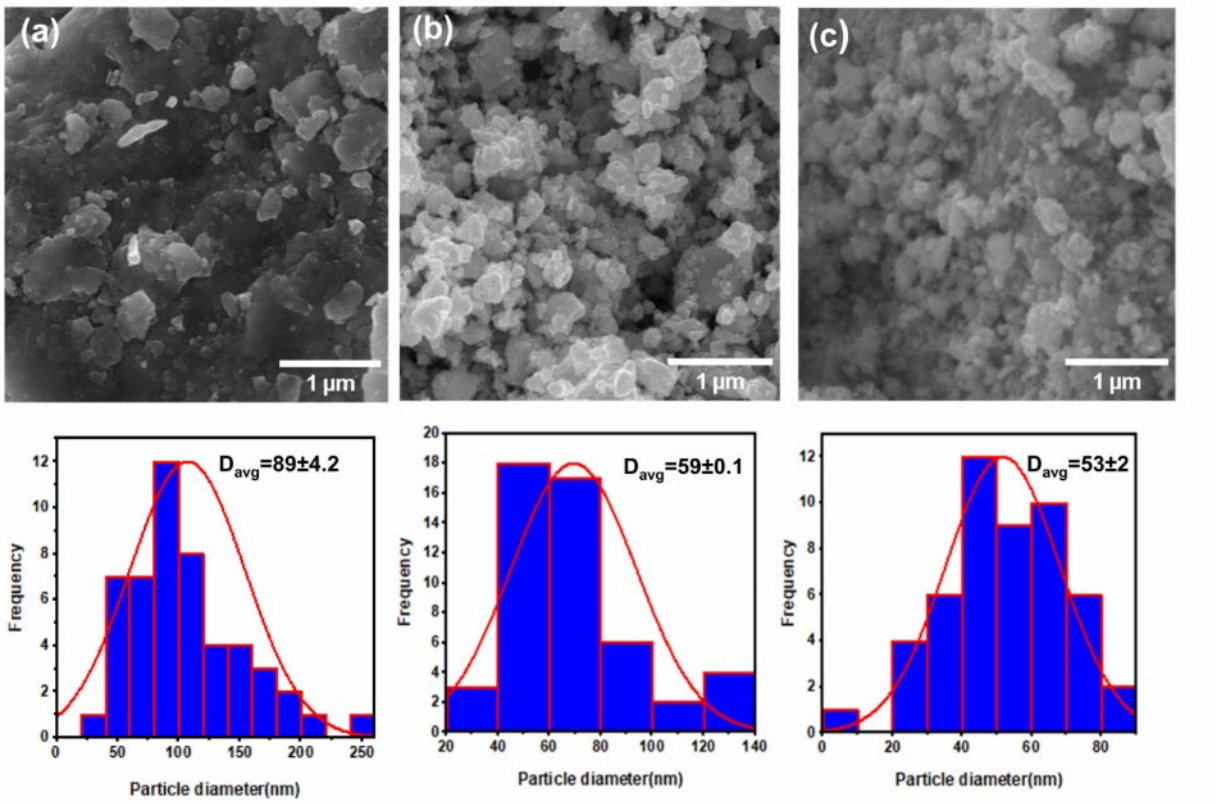

Fig. 2. FE-SEM-secondary electron micrographs, particle size distribution, and average particle size (D_{avg}) of mechanically alloyed (MAed) powders after 30 hours of milling of (a) Pure W, (b) W-1.5wt.%Ir, (c) W-1.5wt.%Ir-2Y_2O_3.

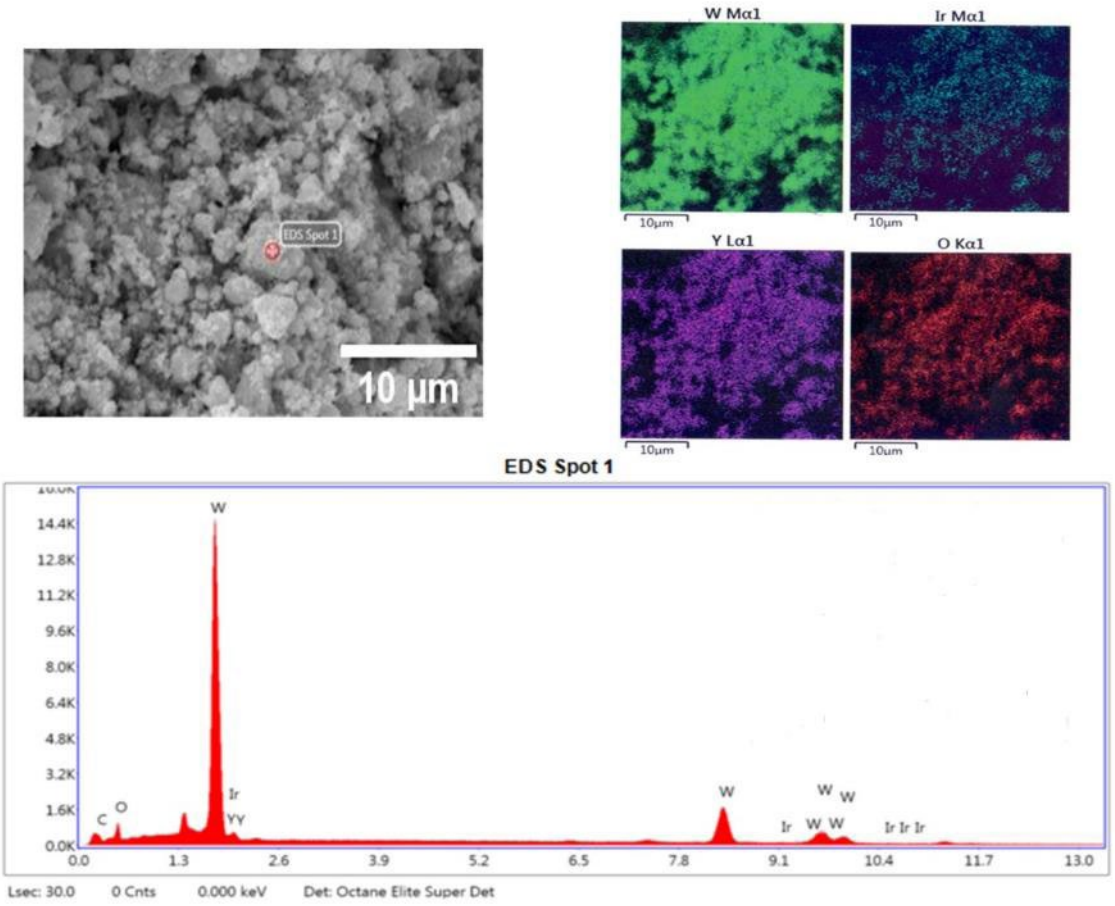

Fig. 3. Energy dispersive X-ray (EDX) analysis and elemental mapping of mechanically alloyed (MAed) W-1.5wt. %Ir-2Y_2O_3 composite powder.

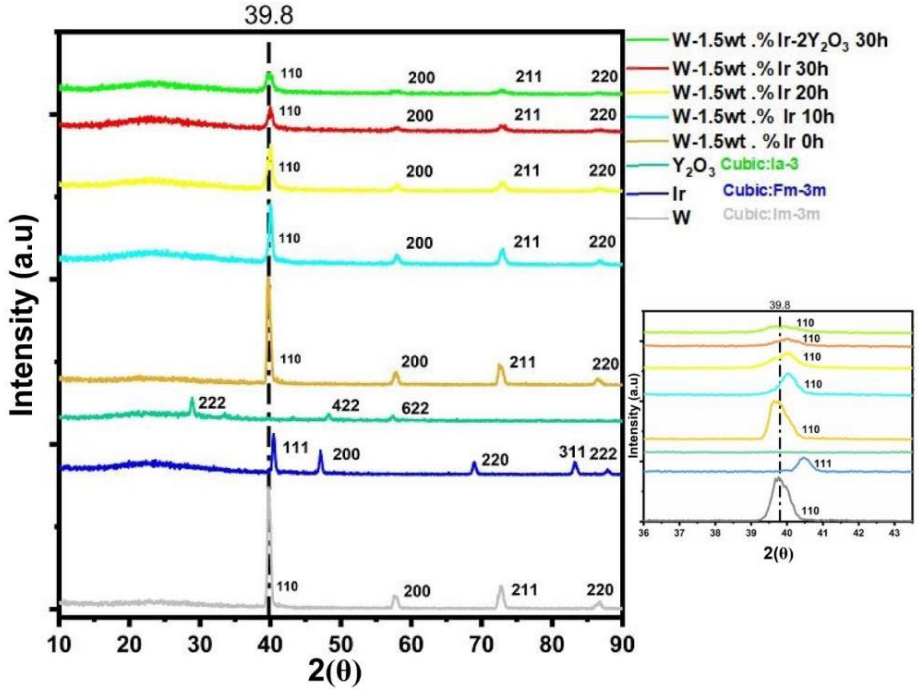

Fig. 4. X-ray diffraction (XRD) patterns of W-1.5 wt.% Ir alloy and W-1.5wt.% Ir-2Y_2O_3 composite mechanically alloyed (MAed) for 30 hours.

Table 1. Crystallite size, lattice strain, dislocation density, and particle size of 30 hours mechanically alloyed (MAed) powders.

Sample name	Crystallite size (nm)	Dislocation density (δ/m^2)	Lattice strain (ε) x10^{-3}	Average particle size (D_{avg}: nm)
Pure W	13.2	1.52918E+15	4.49	89±4.2
W-1.5wt. %Ir	12.5	6.25028E+15	9.1	59±0.1
W-1.5wt. %Ir-2Y_2O_3	11.9	1.42329E+16	13.82	53±2

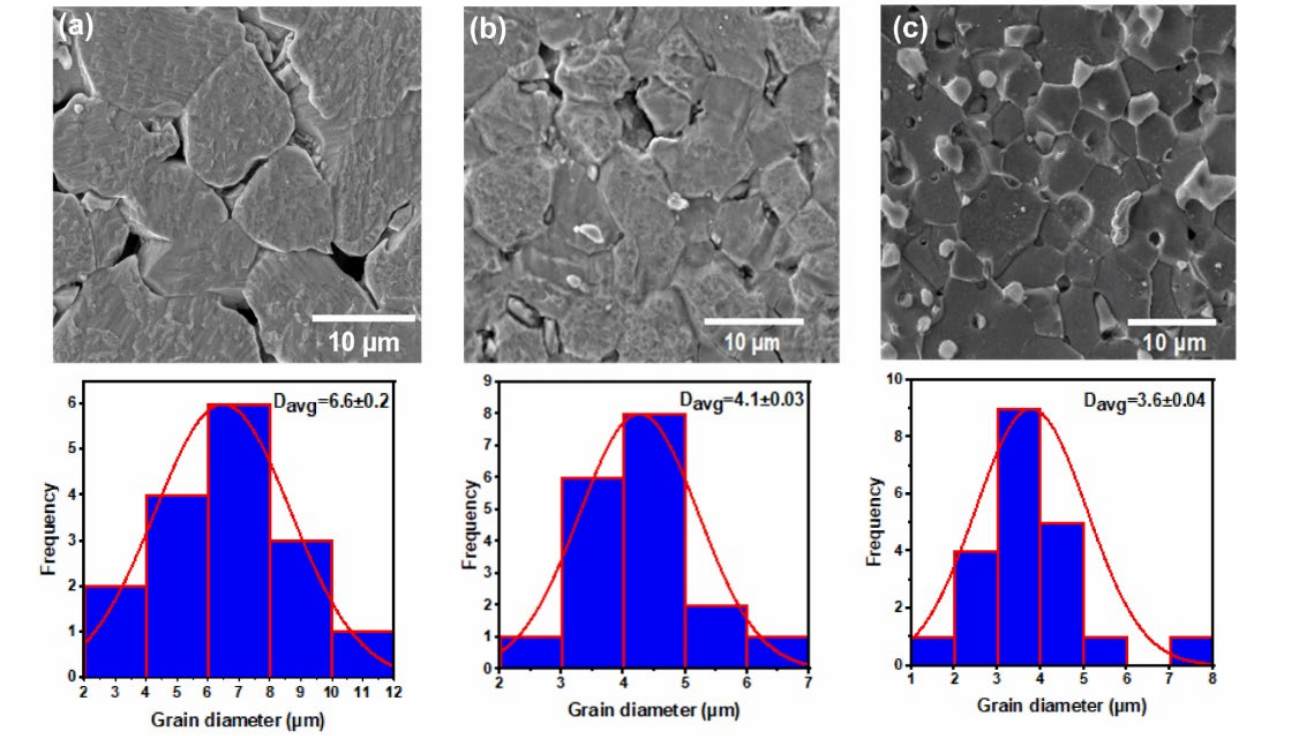

Fig. 5. FE-SEM Secondary electron (SE) micrographs, particle size distribution, and average grain sizes (Davg) of spark plasma sintered (SPSed) (a) Pure W, (b) W-1.5wt. % Ir alloy and (c) W-1.5wt. %Ir-2Y2O3 composite materials.

The relative densities of all SPS treated compacts are shown in the Table 2. It clearly shows that among all the consolidated samples, composite had higher relative density, followed by the alloy and pure tungsten. The higher sinterability of the composites and alloys can be attributed to the smaller starting crystallite/particle sizes obtained after 30 hours of milling. This increases the grain boundary area and defect concentration within the material and promotes atomic diffusion, thereby improving sinter ability. The higher sinterability in tungsten alloys as compared to pure tungsten has been reported earlier for given alloy systems of W-Re ,W-La_2O_3, and W-Y_2O_3 respectively [57,58]. Figure 5a and Table 2 illustrated that pure tungsten is consolidated with large grain size of 6.6±0.2µm, showed large porosity and less continuity among the grains, respectively. On the other hand, the alloy and composite exhibited a finer microstructure than pure tungsten, with minimal porosity or higher relative densities, and average grain sizes are in the ranges of 4.1±0.03µm and 3.6±0.04µm respectively (Figure 5b, c, and Table 2, respectively).The contiguity of the alloy and composite grains is better than that of pure tungsten, indicating the improved sinterability of these materials.

The decrease in grain size of the tungsten-iridium alloy can be attributed to the solid solution strengthening effect of iridium at elevated temperatures, which enhances the thermal stability of the grains. The microstructural refinement of tungsten via alloying is also reported in earlier studies in given alloy systems e.g. W-V (Martínez et al. 2013),W-Ti8(Muñoz et al. 2014), W-Ta, W-Re (Watanabe et al. 2019; Luo et al. 2016),W-Y(Lemahieu et al. 2014), and W-Zr (Xie et al. 2014; Liu et al. 2014) etc. Similarly, for composite the reduction in grain size may be due to pinning effect by second phase fine yttrium oxide particles. Additionally, these oxide particles can interact with free oxygen to purify and hence strengthen the grain boundaries (Z. Wu et al. 2023). The strengthening of tungsten with addition of second phase hard particles at high temperature is also observed in previous studies (Skoczylas and Kaczorowski 2021; Liu et al. 2016; Hesabi et al. 2013; Zhou et al. 2012).

The uniform distribution and fine-grained nature of these second phase yttria particles improves the mechanical properties (wear and hardness) as discussed below.

Similarly, XRD pattern of all SPS-treated samples revealed that the peaks of all sintered specimens became sharper, narrower, and more intense than the corresponding milled powders (Figure 7). This can be attributed to the growth of very fine and strained mechanically alloyed powders (Table 1). Furthermore, as illustrated in Fig. 7, both the W-1.5wt.%Ir alloy and the W-1.5wt.%Ir -2Y2O3 composite exhibit peak splitting and a shift towards higher angles. Moreover, several minor peaks are also present in their experimental XRD patterns. By comparing the reflections of different possible phases of W-Ir-Y-O-C system with the experimental XRD patterns of W-1.5 wt. % Ir and W-1.5 wt. % Ir-Y_2O_3 systems, different phases of IrWO, YWC_2, and WO_3 are being identified. Similar phases of complex mixed oxides and carbides have also been appeared in the W-Y_2O_3, WO_3-Y_2O_3, WO_3-C, and WC-Ir systems, and reported in previous studies(Duerrschnabel et al. 2020; Rybin et al. 2019)

The elemental maps of W, Ir, O, Y, and C confirmed the presence of these elements in consolidated W 1.5wt.%Ir-2Y_2O_3 composite compact. Figure 6f and d depicted that the mapping of Y and O did not overlap, that means yttria didn't present in Y_2O_3 form, instead distributed into different phases as identified in Figure 7 because of possible phase reaction during sintering as described above. In Table 2 a slight increase of crystallite size for composites was noticed, indicating the higher sinterability compared to alloys, which reduces defects and increases regular crystal unit cells or crystallinity.

Figure 8 evident that the addition of iridium to tungsten enhances hardness, reduces the coefficient of friction, and improves the specific wear rate. This might be attributed to enhanced densification, reduction in grain size, and solid solution strengthening effect. The improvement of hardness and tribological properties of tungsten due to iridium is consistent with other studies (Setyawan and Kurtz 2012; Arshad et al. 2014) which shows that the improvement in mechanical properties of tungsten with addition of high d band electrons is due to better cohesion of tungsten matrix at the grain boundaries. Similarly, further enhancement of hardness, reduction in coefficient of friction, and wear rate was observed in case of composite as compared to alloy and pure tungsten (Figure 8). This improvement in tribological behavior might be attributed to following factors; further reduction in grain size of composite, higher sinter ability, and presence of second phase fine hard yttria particle situated at grain boundaries of W-Ir

alloy matrix , and imparted strengthening to matrix due to grain boundaries pinning action likewise other oxide (Y_2O_3, La_2O_3, and HfO_2) and carbides (ZrC, HfC, WC, and TiC) particles (Xie et al. 2015; Fan et al. 2014; Bose, Sadangi, and German 2012; German, Meyer, and Ei-desouky 2012).

2D optical profilometry is a versatile and non-contact technique used to characterize the topography of to worn surfaces with high accuracy and resolution. It measures the roughness profile of the worn surface to obtain the different amplitude parameters such as R_p, R_v, R_z, and R_a as depicted in Figure 9. These parameters provide insight about surface topography. From Amplitude –roughness profile one can quantify the wear in materials. The parameter R_z makes it possible to discriminate two surfaces by comparing their maximum height. A rough surface will have larger R_z value than the corresponding smooth surface. For example, a large value of either R_p and R_v indicates deep grooves or valleys due to scratches and debris or are present on surfaces. This implies that severe wear is happened in materials.

Optical profiles of worn surfaces for pure tungsten, tungsten-iridium alloy, and tungsten iridium-yttria composite were measured as shown in Figure 10a-c and their values presented in Table 3. From Table 3 it can be seen that R_z, and R_a value for pure tungsten compact found to be higher than W-1.5wt. % Ir alloy and W-1.5wt. %Ir-2Y_2O_3 composite. This shows that large debris (height) and deep grooves/scratches (valleys) are present on the surface of pure tungsten than alloy and composite, which are also confirmed by large track width in FE-SEM-micrograph (Figure 11a). Additionally, the higher average roughness value of pure tungsten indicated less smoothness of surface. The mean height of the valley or grooves from mean lines can be measured and shown in Figure 10a-c and Figure 3, where it can be observed that pure tungsten has higher mean height value than rest of alloy and composite samples.

To understand the wear mechanisms, the FE- SEM morphologies of the wear scars produced after wear of samples were examined, as illustrated in Figure 11a-c. After wear test at RT (Figure 11a) there is large track width of 500 micron and larger COF value of 0.32, which reveals an adhesive wear mechanism. High COF value results into welding of and subsequent cutting of surfaces because of poor due to lubrication. The fragmentation of surface into very large number of wear debris indicates brittle nature of tungsten at RT. The higher wear rates can be

Table 2. Density, crystallite, and grain sizes of spark plasma sintered (SPSed) compacts.

Sample name	Theoretical density (g/cm^3)	Archimedes density (g/cm^3)	Relative density (%)	Crystallite size (nm)	Average grain size (D_{avg}: µm)
Pure W	19.34	16.1±0.6	83.2	39	6.6±0.2
W-1.5 wt.% Ir	19.38	17.4±0.5	90	33.5	4.1±0.03
W-1.5wt. %Ir-2Y_2O_3	18.1	17.7±0.4	97.7	33.8	3.6±0.04

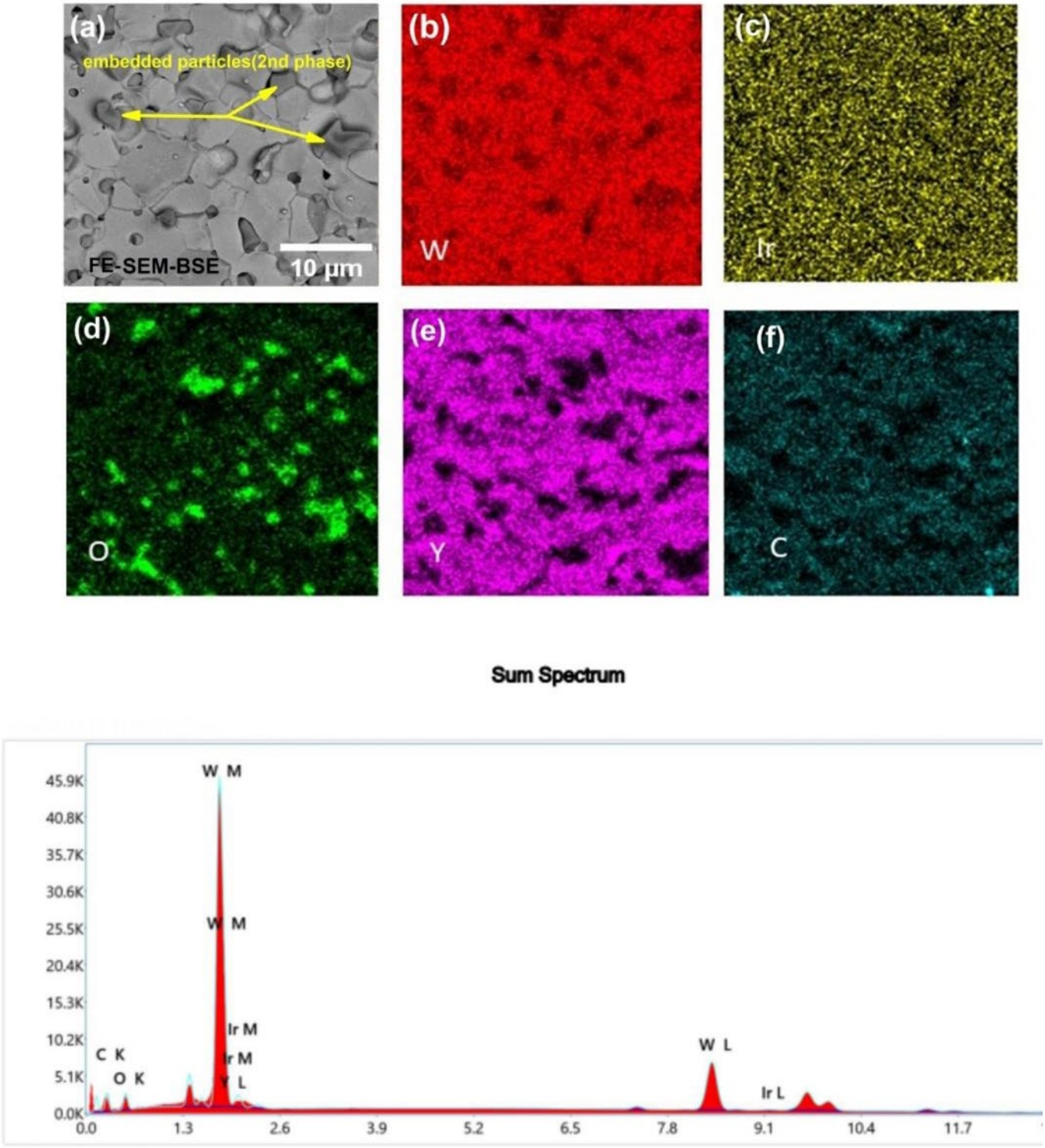

Fig. 6. Elemental maps of W, Ir, O, Y, and C elements and EDX analysis of spark plasma sintered (SPSed) W-1.5wt. %Ir-2Y2O3 composite compact.

attributed to large porosity and large grains size. This rises the surfaces temperature due to frictional heat as well as reduces strength and consequently leads higher wear rate e.g.6.2 ×10−5mm3/Nm. Similarly, from EDS analysis the presence of oxygen in wear debris , indicates the occurrence of oxidative wear mechanism. FE-SEM analysis of the worn surface of W-1.5 wt.% Ir alloy shows that, generation of large number of scattered debris, a wear track width 290 micron, and COF value 0.2, indicated the sample experienced severe adhesive wear like pure tungsten. This is due to higher porosity effect (Table 2), which makes the pin-alloy adhere and results in large mass loss. The EDS analysis further revealed that wear debris are composed of W and Ir atoms which implies that no oxidative wear has happened due to high oxidation resistance induced by iridium to tungsten. For W-1.5wt. %Ir-2Y2O3 composite the wear rate decreased largely to 2.5× 10−5 mm3 /N m. The presence of yttrium oxide, other complex oxides, and carbide , as indicated in the EDS analysis in fig.6-and by XRD analysis in Figure 7,reduced the wear of material due to lubricating effect by these oxide or carbide phases oxide layer[(Roy et al. 2023)(Aouadi et al. 2014)].These oxides reduces the COF value to 0.02,which contributed to the wear resistance. The increase of hardness due to W-1.5 wt.% Ir-2Y2O3 composite, is also responsible for its higher wear resistance than rest of alloy and pure tungsten. The worn surface analysis shows more scratches are present on surface along the sliding direction, as seen in Figure 11c, indicates the abrasive wear is the dominant wear mechanism.

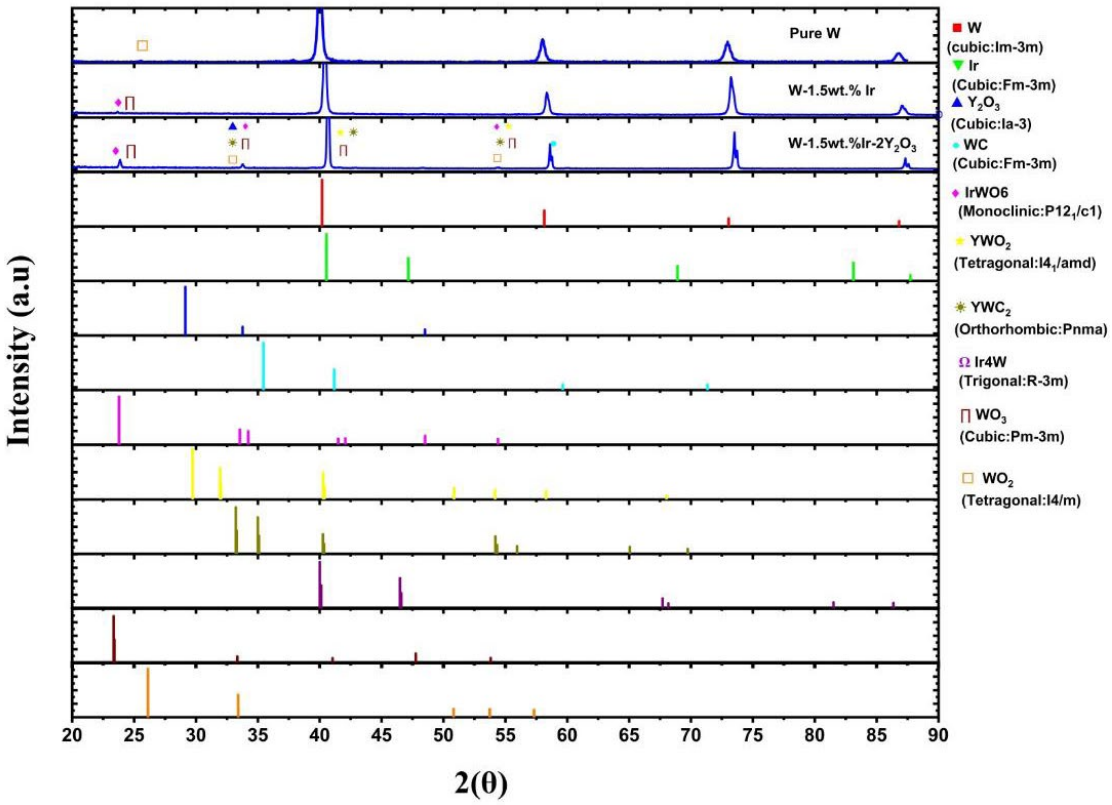

Fig. 7. Phase identification and X-ray diffraction measurements of spark plasma sintered (SPSed) pure W, W-1.5wt. % Ir alloy and W-1.5wt. %Ir-2Y_2O_3 composite compacts.

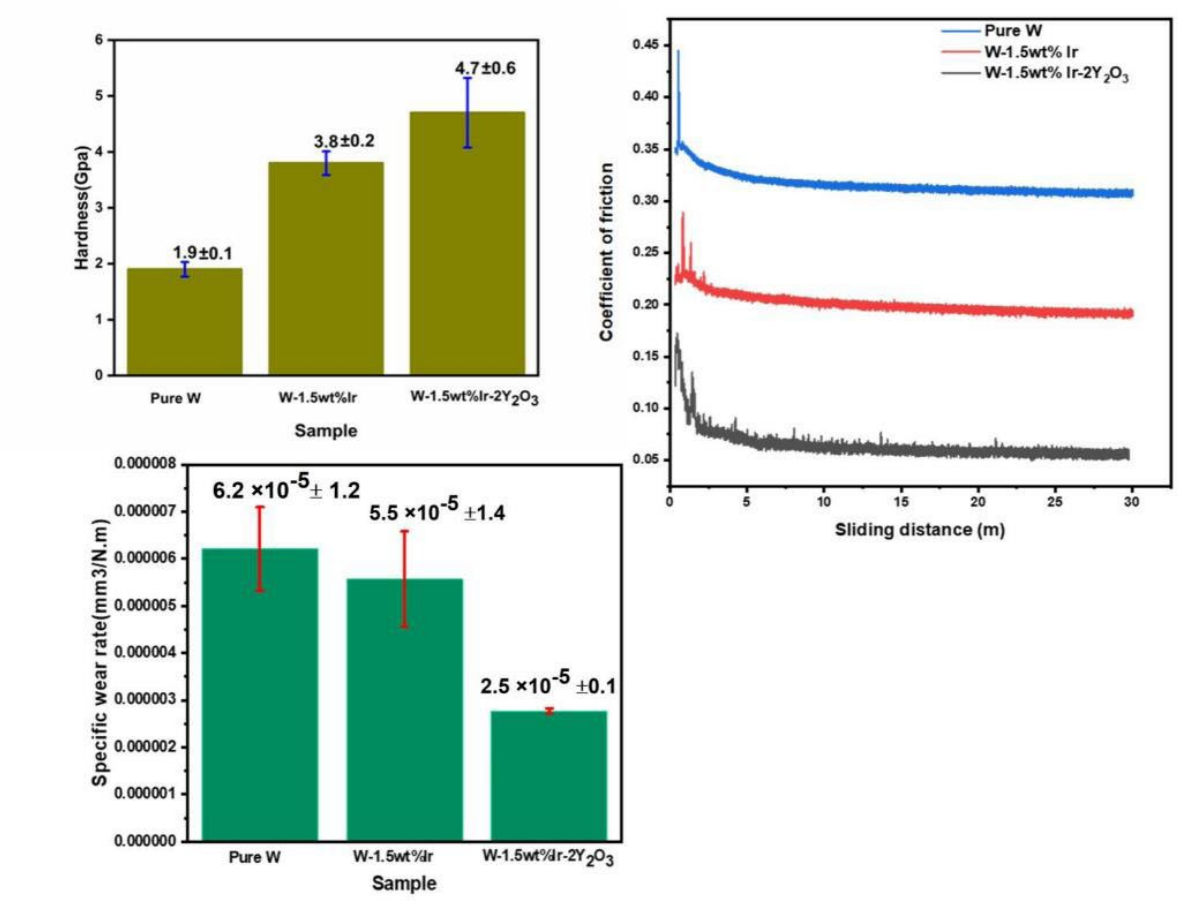

Fig. 8. Hardness, Coefficient of friction, and specific wear rate of Pure W, W-1.5wt. % Ir alloy and W-1.5wt. %Ir-2Y_2O_3 composite compacts.

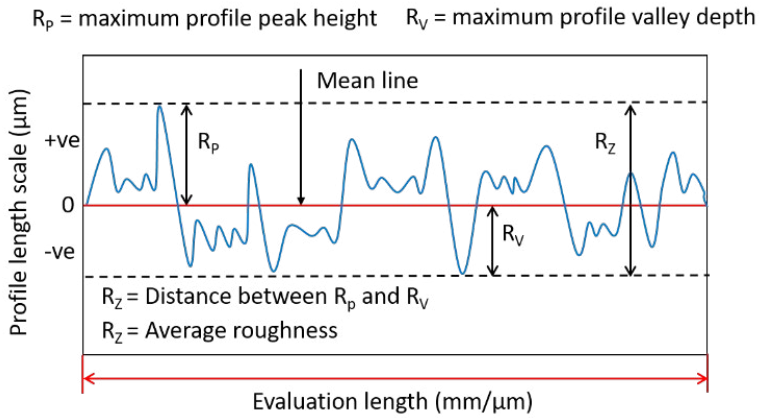

Fig. 9. Schematic of roughness profile and its various parameters.

Table 3. ISO 4287 Amplitude parameter of roughness profile for Pure W, W-1.5wt. %Ir, and W-1.5wt. %Ir-2Y_2O_3 materials

Parameter (µm)	Sample		
	Pure W	W-1.5wt. %Ir alloy	W-1.5wt. %Ir-2Y_2O_3 composite
R_a	2.31	1.83	0.604
R_v	2.11	1.33	0.673
R_z	4.42	3.16	1.28
R_a	0.860	0.519	0.289
Groove mean height	12.1	9.58	3.77

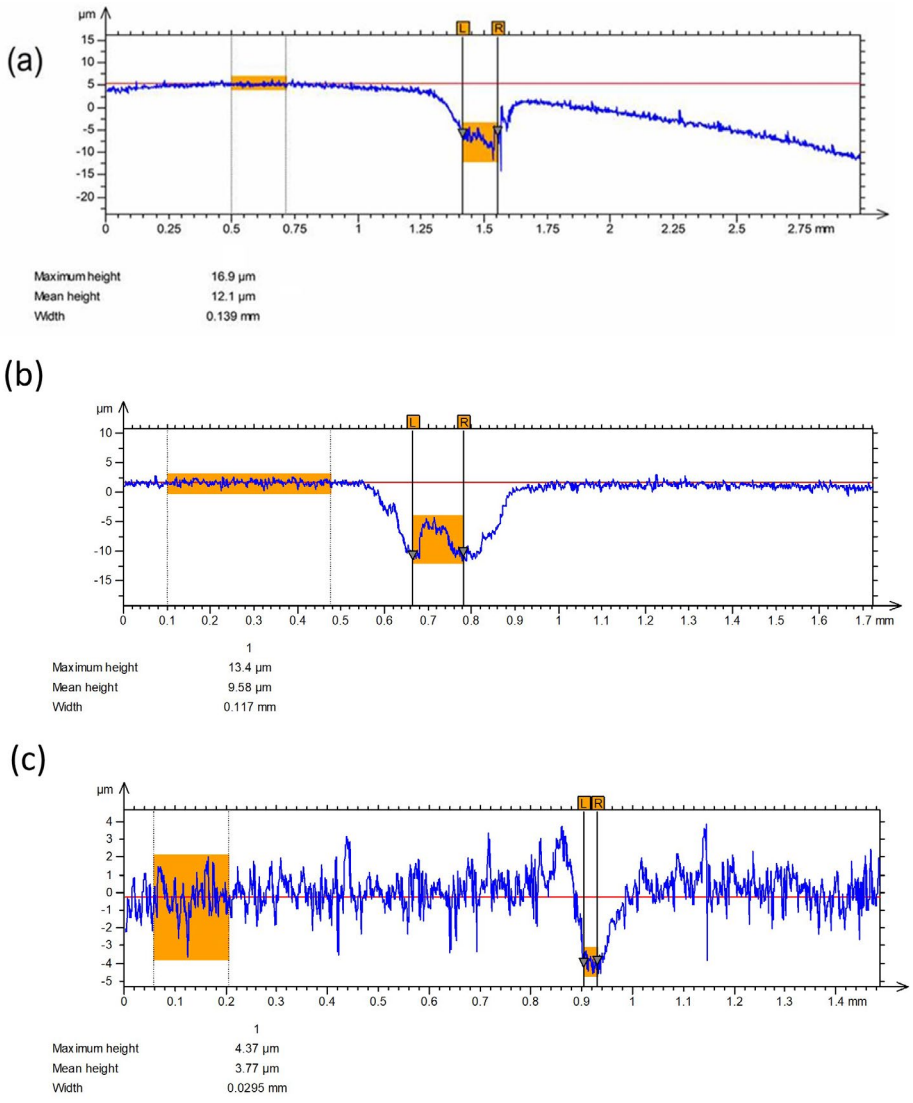

Fig. 10. 2D-Optical profiles (experimental) of (a) pure W, (b) W-1.5wt. % Ir alloy and (c) W-1.5wt. %Ir-2Y2O3 composite compacts.

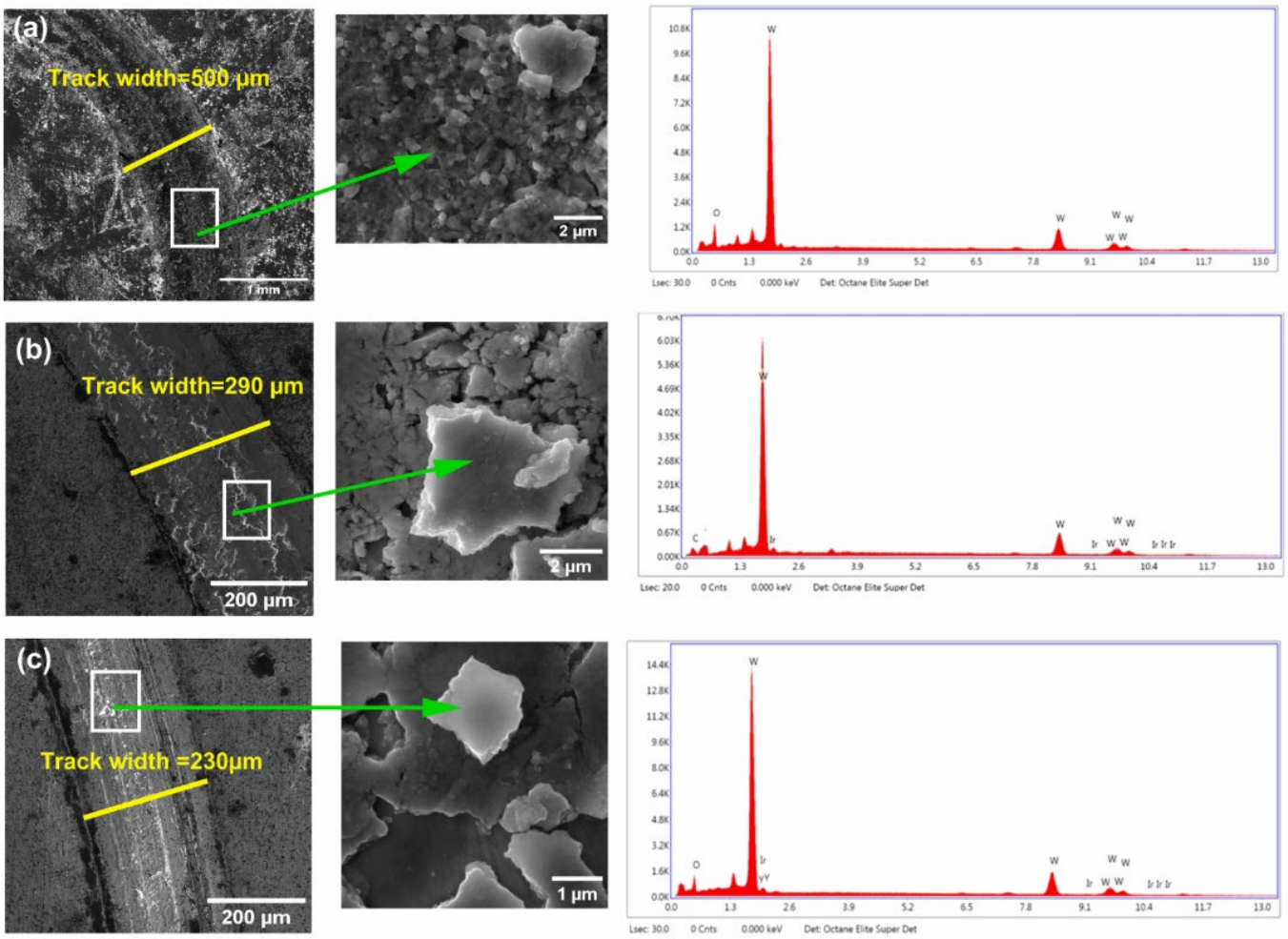

Fig. 11. FE-SEM/EDX analysis of wear track and wear debris for spark plasma sintered (SPSed) (a) Pure W, (b) W-1.5wt.%Ir alloy, and (c) W-1.5wt.%Ir-2Y_2O_3 composite compacts.

4. Conclusion

The successful preparation of pure tungsten, W-1.5 wt.% alloy, and W-1.5 wt.% Ir-2Y_2O_3 composite materials was achieved using spark plasma sintering of mechanically alloyed powders. The pure tungsten sample exhibited inadequate grain bonding leading to low densification, and inferior properties like wear resistance and hardness. In contrast, incorporating iridium into tungsten enhances the interconnectivity of the grains and increases densification from 83.2% to 90%, refines the grain size from 6.6µm to 4.1µm, and results in improvement of wear properties. Similarly, the addition of yttria particles to the tungsten-iridium alloy matrix showed good bonding among grains and enhancement of densification from 90%. to 98%, refinement of grain size from 4.1 µm to 3.6 µm, and uniform distribution of second phase oxides/carbide particles. So, W-1.5 wt.% Ir-2Y_2O_3 composite is produced with the best mechanical properties (wear resistance and hardness), suggesting that tungsten-based materials can be applied reliably into many applications such as a future tool material for friction stir welding/processing of high temperature materials.

Acknowledgments

The authors would like to acknowledge the financial support provided by Higher Education Commission (HEC) through National Research Program for Universities (NRPU) grant # 10666 for this research work. The authors also acknowledge the technical support received from Pakistan Institute of Engineering and Applied Sciences (PIEAS) and Center of Excellence in Nanotechnology, King Fahd University of Petroleum and Minerals (KFUPM), Saudi Arabia for this project.

References

Alloys, W-ni-fe. 2016. “Microwave Sintering of Refractory Metals / Alloys : Microwave Sintering of Refractory Metals / Alloys : W , Mo , Re , W-Cu , W-Ni-Cu and W-Ni-Fe Alloys” 7823 (August): 28–44. https://doi.org/10.1080/08327823.2010.11689768.

Aouadi, S. M., H. Gao, A. Martini, T. W. Scharf, and C. Muratore. 2014. “Lubricious Oxide Coatings for Extreme Temperature Applications: A Review.” *Surface and Coatings Technology*. https://doi.org/10.1016/j.surfcoat.2014.05.064.

Arshad, Kameel, Ming Yue Zhao, Yue Yuan, Ying Zhang, Zhen Hua Zhao, Bo Wang, Zhang Jian Zhou, and Guang Hong Lu. 2014. “Effects of Vanadium Concentration on the Densification, Microstructures and Mechanical Properties of Tungsten Vanadium Alloys.” *Journal of Nuclear Materials* 455 (1–3). https://doi.org/10.1016/j.jnucmat.2014.04.019.

Ayodele, Olusoji Oluremi, Mxolisi Brendon Shongwe, Peter Apata Olubambi, Babatunde Abiodun Obadele, and Thabiso Langa. 2018. “Hybrid Spark Plasma Sintering of Materials: A Review.” *International Journal of Materials, Mechanics and Manufacturing* 6 (6): 360–64. https://doi.org/10.18178/ijmmm.2018.6.6.407.

Barua, Abhishek, Swastik Pradhan, Manisha Priyadarshini, Aman Patra, and Kanchan Kumari. 2024. “Recent Advancement in Tungsten Heavy Alloy Processing for Different Industrial Applications.” *Journal of Materials Engineering and Performance*. https://doi.org/10.1007/s11665-024-10449-y.

Basak, Sanghita, Debojyoti Nath, and Ratan Das. 2023. “Analysis of Dominant and Intense XRD Peak of (111) Plane of ZnS Nanocrystals for Microstructural Study through Single Line Voigt Method: Calculated Low Dislocation Density Value Emphasizes Larger Stacking of (111) Plane.” *Journal of Molecular Structure* 1293. https://doi.org/10.1016/j.molstruc.2023.136273.

Blagoveshchenskiy, Yu V., N. V. Isaeva, M. A. Sinaiskiy, A. B. Ankudinov, and V. A. Zelensky. 2018. “Tuning the Properties of Refractory Carbide Nanopowders.” *Inorganic Materials: Applied Research* 9 (5): 924–29. https://doi.org/10.1134/S2075113318050039.

Bose, Animesh, Rajendra Sadangi, and Randall M. German. 2012. “A Review on Alloying in Tungsten Heavy Alloys.” *TMS Annual Meeting* 1: 455–65. https://doi.org/10.1002/9781118356074.ch59.

Chanthapan, S., A. Kulkarni, J. Singh, C. Haines, and D. Kapoor. 2012. “Sintering of Tungsten Powder with and without Tungsten Carbide Additive by Field Assisted Sintering Technology.” *International Journal of Refractory Metals and Hard Materials*

31. https://doi.org/10.1016/j.ijrmhm.2011.09.014.

Chen, Chun Liang, and Sutrisna. 2022. "Development of ODS Tungsten Heavy Alloys Reinforced with Co9Al8W Superalloy Binder by Mechanical Alloying." *Journal of Alloys and Compounds* 903. https://doi.org/10.1016/j.jallcom.2022.163762.

Chiteka, Kudzanayi. 2013. "Friction Stir Welding/Processing Tool Materials and Selection." *International Journal of Engineering and Technology* 2 (11): 8–18.

Debata, M., Sengupta, P., Mandal, S., Adhikari, D. n.d. "Consolidation of Tungsten-Heavy Alloys." In *Mechanically Alloyed Novel Materials*., edited by Shashanka Rajendrachari, 1st ed., 235–256. Springer Singapore. https://doi.org/https://doi.org/10.1007/978-981-97-6504-1.

Deng, H. W., Z. M. Xie, Y. K. Wang, R. Liu, T. Zhang, T. Hao, X. P. Wang, Q. F. Fang, and C. S. Liu. 2018. "Mechanical Properties and Thermal Stability of Pure W and W-0.5 Wt%ZrC Alloy Manufactured with the Same Technology." *Materials Science and Engineering: A* 715. https://doi.org/10.1016/j.msea.2017.12.112.

Deng, Shenghua, Tiechui Yuan, Ruidi Li, Fanhao Zeng, Guanghong Liu, and Xiang Zhou. 2017. "Spark Plasma Sintering of Pure Tungsten Powder: Densification Kinetics and Grain Growth." *Powder Technology* 310: 264–71. https://doi.org/10.1016/j.powtec.2017.01.050.

Dong, Zhi, Nan Liu, Weiqiang Hu, Xiangwei Kong, Zongqing Ma, and Yongchang Liu. 2019. "The Effect of Y2O3 on the Grain Growth and Densification of W Matrix during Low Temperature Sintering: Experiments and Modelling." *Materials & Design* 181: 108080. https://doi.org/10.1016/j.matdes.2019.108080.

Dong, Zhi, Nan Liu, Zongqing Ma, Chenxi Liu, Qianying Guo, and Yongchang Liu. 2017. "Preparation of Ultra-Fine Grain W-Y2O3 Alloy by an Improved Wet Chemical Method and Two-Step Spark Plasma Sintering." *Journal of Alloys and Compounds* 695: 2969–73. https://doi.org/10.1016/j.jallcom.2016.11.364.

Duerrschnabel, Michael, Steffen Antusch, Birger Holtermann, Ute Jaentsch, Siegfried Baumgaertner, Carsten Bonnekoh, Mirjam Hoffmann, Jan Hoffmann, and Michael Rieth. 2020. "Elucidating the Microstructure of Tungsten Composite Materials Produced by Powder Injection Molding." *Nuclear Materials and Energy* 24 (June): 100766. https://doi.org/10.1016/j.nme.2020.100766.

EN ISO 3369. 2010. "Impermeable Sintered Metal Materials and Hardmetals - Determination of Density (ISO 3369:2006)." *BSI Standards Publication*.

Fan, Jinglian, Yong Han, Pengfei Li, Zhiyu Sun, and Qiang Zhou. 2014. "Micro/Nano Composited Tungsten Material and Its High Thermal Loading Behavior." *Journal of Nuclear Materials* 455 (1): 717–23. https://doi.org/10.1016/j.jnucmat.2014.09.037.

Froes, F. H., C. R. Clark, C. Suryanarayana, E. G. Baburaj, and B. D. Bryskin. 1998. "Formation of W-Re Solid Solution by Mechanical Alloying." *Materials and Manufacturing Processes* 13 (5): 657–70. https://doi.org/10.1080/10426919808935291.

German, Randall M. 2015. "Lower Sintering Temperature Tungsten Alloys for Space Research." *International Journal of Refractory Metals and Hard Materials* 53: 74–79. https://doi.org/10.1016/j.ijrmhm.2015.04.020.

German, Randall M, John L Meyer, and Ahmed Ei-desouky. 2012. "TIMIS2012."

Goto, Masahiro, Akira Kasahara, and Masahiro Tosa. 2006. "Low Frictional Property of Copper Oxide Thin Films Optimised Using a Combinatorial Sputter Coating System." In *Applied Surface Science*. Vol. 252. https://doi.org/10.1016/j.apsusc.2005.03.236.

Hayden, H. W., and J. H. Brophy. 1963. "The Activated Sintering of Tungsten with Group VIII Elements." *Journal of the Electrochemical Society* 110 (7): 805–10. https://doi.org/10.1149/1.2425876.

Heo, Youn Ji, Eui Seon Lee, Jeong Hyun Kim, Young In Lee, Young Keun Jeong, and Sung Tag Oh. 2022. "Synthesis and Characterization of W Composite Powder With La2O3-Y2O3 Nano-Dispersoids By Ultrasonic Spray Pyrolysis." *Archives of Metallurgy and Materials* 67 (4): 1507–10. https://doi.org/10.24425/amm.2022.141083.

Hesabi, Z R, S Kamrani, A Simchi, S M S Reihani, Z R Hesabi, S Kamrani, A Simchi, and S M S Reihani. 2013. "Effect of Nanoscaled Reinforcement Particles on the Structural Evolution of Aluminium Powder during Mechanical Milling Effect of Nanoscaled Reinforcement Particles on the Structural Evolution of Aluminium Powder during Mechanical Milling" 5899. https://doi.org/10.1179/174329007X189658.

Iqbal, Zafar, Nouari Saheb, and Abdel Rahman. 2016. "W-25 % Re-HfC Composite Materials for Pin Tool Material Applications : Synthesis and Consolidation." *Journal of Alloys and Compounds* 674: 189–99. https://doi.org/10.1016/j.jallcom.2016.03.030.

Karafi, Toufik, Abdellah Tahiri, Mouhamed Idiri, Chabba Chabba, and Brahim Boubeker. 2023. "EFFECT THE CONCENTRATION OF RHENIUM ON THE MECHANICAL PROPERTIES AND DISLOCATION MECHANISMS OF TUNGSTEN-RHENIUM ALLOY." *International Journal on Technical and Physical Problems of Engineering* 15 (4).

Kiran, U Ravi, A Panchal, M Prem Kumar, M Sankaranarayana, G V S Nageswara Rao, and T K Nandy. 2017. "Refractory Metal Alloying: A New Method for Improving Mechanical Properties of Tungsten Heavy Alloys." *Journal of Alloys and Compounds*. https://doi.org/10.1016/j.jallcom.2017.03.174.

Lakshmi Prasad, B. S., and A. Raja Annamalai. 2021. "Effect of Rhenium Addition on Tungsten Heavy Alloys Processed through Spark Plasma Sintering." *Ain Shams Engineering Journal* 12 (3). https://doi.org/10.1016/j.asej.2021.02.022.

Lang, E., X. Wang, R. Kolasinski, and J. P. Allain. 2025. "Dispersion-Strengthened Tungsten Alloy Composites." *Fusion Energy Technology R and D Priorities*, January, 65–69. https://doi.org/10.1016/B978-0-443-13629-0.00008-3.

Lau, Alexander, Jan Willem Coenen, Daniel Schwalenberg, Yiran Mao, Till Höschen, Johann Riesch, Leonard Raumann, et al. 2023. "Bulk Tungsten Fiber-Reinforced Tungsten (Wf/W) Composites Using Yarn-Based Textile Preforms." *Journal of Nuclear Engineering* 4 (2): 375–90. https://doi.org/10.3390/jne4020027.

Lee, Dongju, Malik Adeel Umer, Ho J. Ryu, and Soon H. Hong. 2014. "The Effect of HfC Content on Mechanical Properties HfC-W Composites." *International Journal of Refractory Metals and Hard Materials* 44: 49–53. https://doi.org/10.1016/j.ijrmhm.2014.01.012.

Lee, Eui Seon, Youn Ji Heo, Young In Lee, Young Keun Jeong, and Sung Tag Oh. 2022. "Microstructural Characterization and Densification of W-1 Wt% La2O3 Composite Powders Synthesized by Ultrasonic Spray Pyrolysis." *Journal of Materials Science* 57 (38): 17946–56. https://doi.org/10.1007/s10853-022-07478-0.

Lee, G, J Mckittrick, E Ivanov, and E A Olevsky. 2016. "Int . Journal of Refractory Metals and Hard Materials Densi Fi Cation Mechanism and Mechanical Properties of Tungsten Powder Consolidated by Spark Plasma Sintering." *RMHM* 61: 22–29. https://doi.org/10.1016/j.ijrmhm.2016.07.023.

Lee, Jin-kyu, Song-yi Kim, Ryan T Ott, Jin-young Kim, and Min-ha Lee. n.d. "Effect of Reinforcement Phase on the Mechanical Property of Tungsten Nanocomposite Synthesized by Spark Plasma Sintering," 1–19.

Lemahieu, N., J. Linke, G. Pintsuk, G. Van Oost, M. Wirtz, and Z. Zhou. 2014. "Performance of Yttrium Doped Tungsten under 'Edge Localized Mode'-like Loading Conditions." In *Physica Scripta*. Vol. T159. https://doi.org/10.1088/0031-8949/2014/T159/014035.

Li, Lulu, Zhi Dong, Zongqing Ma, Chenxi Liu, Liming Yu, and Yongchang Liu. 2023. "Ultrahigh Strength and Toughness in W-Y2O3 Alloy with Bimodal and Lamellar Structures." *Materials Research Letters* 11 (6): 439–45. https://doi.org/10.1080/21663831.2023.2181110.

Li, Tong, Tianwei Liu, Shiteng Zhao, Yan Chen, Junhua Luan, Zengbao Jiao, Robert O. Ritchie, and Lanhong Dai. 2023. "Ultra-Strong Tungsten Refractory High-Entropy Alloy via Stepwise Controllable Coherent Nanoprecipitations." *Nature Communications* 14 (1): 1–7. https://doi.org/10.1038/s41467-023-38531-4.

Li, Xiaojing, Hanli Liu, Peng Hu, Jinshu Wang, Yunfei Yang, Hongyi Li, and Wenyuan Zhou. 2022. "Nanostructured TiC Dispersion-Strengthened Tungsten Composite with Remarkably Improved He Ion Irradiation Resistance." *International Journal of Refractory Metals and Hard Materials* 107 (September): 105900. https://doi.org/10.1016/J.IJRMHM.2022.105900.

Liu, R, Z M Xie, Q F Fang, T Zhang, X P Wang, T Hao, C S Liu, and Y Dai. 2016. "Nanostructured Yttria Dispersion-Strengthened Tungsten Synthesized by Sol e Gel Method." *Journal of Alloys and Compounds* 657: 73–80. https://doi.org/10.1016/j.jallcom.2015.10.059.

Liu, R, Z M Xie, T Hao, Y Zhou, X P Wang, Q F Fang, and C S Liu. 2014. "Fabricating High Performance Tungsten Alloys through Zirconium Micro-Alloying and Nano-Sized Yttria Dispersion Strengthening." *JOURNAL OF NUCLEAR MATERIALS* 451 (1–3): 35–39. https://doi.org/10.1016/j.jnucmat.2014.03.029.

Liu, R, Z M Xie, J F Yang, T Zhang, T Hao, X P Wang, Q F Fang, and C S Liu. 2018. "Recent Progress on the R & D of W-ZrC Alloys for Plasma Facing Components in Fusion Devices." *Nuclear Materials and Energy* 16 (May): 191–206. https://doi.org/10.1016/j.nme.2018.07.002.

Luo, Laima, Jing Shi, Jinshan Lin, Xiang Zan, Xiaoyong Zhu, Qiu Xu, and Yucheng Wu. 2016. "Microstructure and Performance of Rare Earth Element-Strengthened Plasma-Facing Tungsten Material." *Nature Publishing Group*, no. March: 1–9. https://doi.org/10.1038/srep32701.

Ma, J, and S G Zhu. 2010. "Int . Journal of Refractory Metals and Hard Materials Direct Solid-State Synthesis of Tungsten Carbide Nanoparticles from Mechanically Activated Tungsten Oxide and Graphite" 28: 623–27. https://doi.org/10.1016/j.ijrmhm.2010.06.004.

Marchhart, Trevor, Chase Hargrove, Alexandru Marin, Hanna Schamis, Ashrakat Saefan, Eric Lang, Xing Wang, and Jean Paul Allain. 2024. "Discovering Tungsten-Based Composites as Plasma Facing Materials for Future High-Duty Cycle Nuclear Fusion Reactors." *Scientific Reports* 14 (1): 1–13. https://doi.org/10.1038/s41598-024-64614-3.

Martínez, J., B. Savoini, M. A. Monge, A. Muñoz, D. E.J. Armstrong, and R. Pareja. 2013. "Thermal Stability of the Grain Structure in the W-2V and W-2V-0.5Y 2O3 Alloys Produced by Hot Isostatic Pressing." In *Fusion Engineering and Design*. Vol. 88. https://doi.org/10.1016/j.fusengdes.2013.05.057.

Merker, J., D. Lupton, M. Töpfer, and H. Knake. 2001. "High Temperature Mechanical Properties of the Platinum Group Metals: Elastic Properties of Platinum, Rhodium and Iridium and Their Alloys at High Temperatures." *Platinum Metals Review* 45 (2): 74–82.

Min, Guensik, Yeonju Oh, Hwangsun Kim, Eunjoo Shin, Ki Baek Roh, Jeongseok Kim, Nojun Kwak, et al. 2023. "Effect of Yttrium Doping in Tungsten on Sinterability and Properties as a Plasma-Facing Material." *Journal of Alloys and Compounds* 953. https://doi.org/10.1016/j.jallcom.2023.169961.

Mishra, R.S., and Z.Y. Ma. 2005. "Friction Stir Welding and Processing." *Materials Science and Engineering: R: Reports* 50 (1–2): 1–78. https://doi.org/10.1016/j.mser.2005.07.001.

Muñoz, A., B. Savoini, E. Tejado, M. A. Monge, J. Y. Pastor, and R. Pareja. 2014. "Microstructural and Mechanical Characteristics of W-2Ti and W-1TiC Processed by Hot Isostatic Pressing." *Journal of Nuclear Materials* 455 (1–3). https://doi.org/10.1016/j.jnucmat.2014.06.064.

Nisar, Ambreen, Cheng Zhang, Benjamin Boesl, and Arvind Agarwal. 2021. "Unconventional Materials Processing Using Spark Plasma Sintering." *Ceramics*. https://doi.org/10.3390/ceramics4010003.

Nygren, R. E., R. Raffray, D. Whyte, M. A. Urickson, M. Baldwin, and L. L. Snead. 2011. "Making Tungsten Work - ICFRM-14 Session T26 Paper 501 Nygren et Al. Making Tungsten Work." In *Journal of Nuclear Materials*. Vol. 417. https://doi.org/10.1016/j.jnucmat.2010.12.289.

Oda, Eiji, Kei Ameyama, and Satoru Yamaguchi. 2006. "Fabrication of Nano Grain Tungsten Compact by Mechanical Milling Process and Its High Temperature Properties" 504: 573–78. https://doi.org/10.4028/www.scientific.net/MSF.503-504.573.

Oshrieh, Mohammad Bagher, Karim Zangenemadar, Hasan Abbaszadeh, Meysam Ahangarkani, and Hamedreza Javadian. 2024. "Improvement of Mechanical and Wear Properties of Tungsten Heavy Alloy Using Two-Stage Sintering and Carburizing Processes." *Journal of Materials Engineering and Performance*, no. Ref 22. https://doi.org/10.1007/s11665-024-09782-z.

Parthasarathy, T. A., M. G. Mendiratta, and D. M. Dimiduk. 2002. "Oxidation Mechanisms in Mo-Reinforced Mo5SiB2(T2)-Mo3Si Alloys." *Acta Materialia* 50 (7). https://doi.org/10.1016/S1359-6454(02)00039-3.

Pitts, R. A., S. Carpentier, F. Escourbiac, T. Hirai, V. Komarov, S. Lisgo, A. S. Kukushkin, et al. 2013. "A Full Tungsten Divertor for ITER: Physics Issues and Design Status." *Journal of Nuclear Materials* 438 (SUPPL). https://doi.org/10.1016/j.jnucmat.2013.01.008.

Pramanik, Sudipta, Ajeet K. Srivastav, Bobu Manuel Jolly, Niraj Chawake, and B. S. Murty. 2019. "Effect of Re on Microstructural Evolution and Densification Kinetics during Spark Plasma Sintering of Nanocrystalline W." *Advanced Powder Technology* 30 (11): 2779–86. https://doi.org/10.1016/j.apt.2019.08.025.

Que, Zhongyou, Xingyu Li, Lin Zhang, En Mei, Chenguang Guo, Haishen Sun, Junming Liu, Mingli Qin, Gang Chen, and Xuanhui Qu. 2025. "Preparation and Properties of Tungsten-Rhenium Alloys Resistant to Ultra-High Temperatures." *International Journal of Refractory Metals and Hard Materials* 127 (February): 106975. https://doi.org/10.1016/J.IJRMHM.2024.106975.

R.M .GERMAN, Z.A.MUNIR. 1977. "Rhenium Activating Sintering." *Journal of the Less-Common Metals* 53: 141–46.

Rahul, R, K V Rajulapati, G M Reddy, and K B S Rao. n.d. "Development of Aluminium Based Surface Nano Composites Using Friction Stir Processing," 1–9.

Rai, R., A. De, H. K.D.H. Bhadeshia, and T. DebRoy. 2011. "Review: Friction Stir Welding Tools." *Science and Technology of Welding and Joining* 16 (4): 325–42. https://doi.org/10.1179/1362171811Y.0000000023.

Ren, Chai, Z. Zak Fang, Huan Zhang, and Mark Koopman. 2016. "The Study on Low Temperature Sintering of Nano-Tungsten Powders." *International Journal of Refractory Metals and Hard Materials* 61. https://doi.org/10.1016/j.ijrmhm.2016.10.003.

Riesch, J., A. von Müller, Y. Mao, J. W. Coenen, B. Böswirth, S. Elgeti, M. Fuhr, et al. 2024. "Progress in the Development of Industrial Scale Tungsten Fibre-Reinforced Composite Materials." *Nuclear Materials and Energy* 38 (March): 101591. https://doi.org/10.1016/J.NME.2024.101591.

Roy, Amit, Payank Patel, Navid Sharifi, Richard R. Chromik, Pantcho Stoyanov, and Christian Moreau. 2023. "Binary and Ternary Lubricious Oxides for High Temperature Tribological Applications: A Review." *Results in Surfaces and Interfaces* 11. https://doi.org/10.1016/j.rsurfi.2023.100117.

Rybin, V, V Lozanov, A Utkin, A Matvienko, and N Baklanova. 2019. "The Formation of Disordered Intermetallic Phase during the Solid-State Interaction of WC with Ir." *Journal of Alloys and Compounds* 775: 503–10. https://doi.org/10.1016/j.jallcom.2018.10.118.

Saheb, Nouari, Zafar Iqbal, Abdullah Khalil, Abbas Saeed Hakeem, Nasser Al Aqeeli, Tahar Laoui, Amro Al-Qutub, and René Kirchner. 2012. "Spark Plasma Sintering of Metals and Metal Matrix Nanocomposites: A Review." *Journal of Nanomaterials* 2012. https://doi.org/10.1155/2012/983470.

Samsonov, G. V., and V. I. Yakovlev. 1970. "Activation of the Sintering Process of Tungsten by the Platinum-Group Metals." *Soviet Powder Metallurgy and Metal Ceramics* 9 (1): 30–36. https://doi.org/10.1007/BF00796945.

Setyawan, Wahyu, and Richard J. Kurtz. 2012. "Effects of Transition Metals on the Grain Boundary Cohesion in Tungsten." *Scripta Materialia* 66 (8): 558–61. https://doi.org/10.1016/j.scriptamat.2012.01.002.

Shabalin, Igor L. 2019. *Ultra-High Temperature Materials II. Ultra-High Temperature Materials II*. https://doi.org/10.1007/978-94-024-1302-1.

Shah, V., J. A.W. van Dommelen, E. Altstadt, A. Das, and M. G.D. Geers. 2020. "Brittle-Ductile Transition Temperature of Recrystallized Tungsten Following Exposure to Fusion Relevant Cyclic High Heat Load." *Journal of Nuclear Materials* 541. https://doi.org/10.1016/j.jnucmat.2020.152416.

Siller, M., N. Bostrom, P. Bogust, J. Schatte, S. Gerzoskovitz, H. Clemens, R. Pippan, and V. Maier-Kiener. 2023. "Impact of Microstructure on the Performance of WRe10 Conversion Layers for Stationary and Rotating Anodes." *International Journal of Refractory Metals and Hard Materials* 114 (August): 106244. https://doi.org/10.1016/J.IJRMHM.2023.106244.

Skoczylas, Paweł, and Mieczysław Kaczorowski. 2021. "Preliminary Study of the Rhenium Addition on the Structure and Mechanical Properties of Tungsten Heavy Alloy." *Materials* 14 (23): 34–44. https://doi.org/10.3390/ma14237365.

Snead, Lance L, David T Hoelzer, Michael Rieth, and Andre A N Nemith. 2019. *Chapter 13 - Refractory Alloys: Vanadium, Niobium, Molybdenum, Tungsten. Structural Alloys for Nuclear Energy Applications*. Elsevier Inc. https://doi.org/10.1016/B978-0-12-397046-6.00013-7.

Taillard, R, and J Foct. 2008. "Evolution of Grain Size in Oxide Dispersion Strengthened Tungsten Alloys during Their Elaboration by Ball Milling and Sintering" 5: 669–82.

Thompson, Brian. 2011. "Tungsten-Based Tool Material Development for the Friction Stir Welding of Hard Metals." *TMS Annual Meeting*, 105–12. https://doi.org/10.1002/9781118062302.ch14.

Vaneela, Somisetty. 2017. "DISLOCATION DENSITY IN MULTICOMPONENT ALLOYS CoNi , CoFeNi," 105–10.

Veleva, L., Z. Oksiuta, U. Vogt, and N. Baluc. 2009. "Sintering and Characterization of W–Y and W–Y2O3 Materials." *Fusion Engineering and Design* 84 (7–11): 1920–24. https://doi.org/10.1016/J.FUSENGDES.2008.12.001.

Verma, Krishna Kamlesh, Jitesh Kumar, K. V.Mani Krishna, Shashank Sharma, M. Radhakrishnan, Sameehan S. Joshi, Rajarshi Banerjee, and Narendra Dahotre. 2025. "Effect of Rhenium on Evolution of Microstructure in Tungsten-Rhenium Fabricated by Laser Powder Bed Fusion." *International Journal of Refractory Metals and Hard Materials* 128 (April): 107046. https://doi.org/10.1016/J.IJRMHM.2025.107046.

Wahid, Mohd Atif, Arshad Noor Siddiquee, Zahid Akhtar Khan, and Mohammad Asjad. 2016. "Friction Stir Welds of Al Alloy-Cu: An Investigation on Effect of Plunge Depth." *Archive of Mechanical Engineering* 63 (4): 619–34. https://doi.org/10.1515/meceng-2016-0035.

Wang, R., Z. M. Xie, Y. K. Wang, J. P. Song, Q. F. Fang, R. Liu, Y. Jiang, et al. 2019. "Fabrication and Characterization of Nanocrystalline ODS-W via a Dissolution-Precipitation Process." *International Journal of Refractory Metals and Hard Materials* 80. https://doi.org/10.1016/j.ijrmhm.2019.01.002.

Wang, Yiming, and Jarir Aktaa. 2017. "Microstructure and Texture in W and W-1wt%La2O3 Processed by High-Pressure Torsion." *Scripta Materialia* 139: 22–25. https://doi.org/10.1016/j.scriptamat.2017.06.008.

Wang, Yujin, Hua Xin Peng, Yu Zhou, and Gui Ming Song. 2011. "Influence of ZrC Content on the Elevated Temperature Tensile Properties of ZrCp/W Composites." *Materials Science and Engineering A* 528 (3): 1805–11. https://doi.org/10.1016/j.msea.2010.11.029.

Watanabe, Shotaro, Shuhei Nogami, Jens Reiser, Michael Rieth, Sven Sickinger, Siegfried Baumgärtner, Takeshi Miyazawa, and Akira Hasegawa. 2019. "Tensile and Impact Properties of Tungsten-Rhenium Alloy for Plasma-Facing Components in Fusion Reactor." *Fusion Engineering and Design* 148. https://doi.org/10.1016/j.fusengdes.2019.111323.

Wu, Mingyu, Zhihang Wang, Ningning Zhang, Changchun Ge, and Yujuan Zhang. 2021. "Theoretical Predictions of the Structural and Mechanical Properties of Tungsten-Rare Earth Element Alloys." *Materials* 14 (11). https://doi.org/10.3390/ma14113046.

Wu, Zaoming, Lin He, Linsen Ye, Xiaofeng Yang, Jiajia Zhang, and Hongbo Lei. 2023. "Ultrafine-Grained W-Based Alloys Prepared by HIP with Ultrahigh Hardness and Excellent Thermal Stability." *International Journal of Refractory Metals and Hard Materials* 115. https://doi.org/10.1016/j.ijrmhm.2023.106318.

Xie, Z. M., R. Liu, Q. F. Fang, Y. Zhou, X. P. Wang, and C. S. Liu. 2014. "Spark Plasma Sintering and Mechanical Properties of Zirconium Micro-Alloyed Tungsten." *Journal of Nuclear Materials*. https://doi.org/10.1016/j.jnucmat.2013.09.045.

Xie, Z. M., T. Zhang, R. Liu, Q. F. Fang, S. Miao, X. P. Wang, and C. S. Liu. 2015. "Grain Growth Behavior and Mechanical Properties of Zirconium Micro-Alloyed and Nano-Size Zirconium Carbide Dispersion Strengthened Tungsten Alloys." *International Journal of Refractory Metals and Hard Materials* 51: 180–87. https://doi.org/10.1016/j.ijrmhm.2015.03.019.

Yamabe-mitarai, Yoko, Tomohiro Maruko, Tomoaki Miyazawa, and Tosiyuki Morino. 2005. "Solid Solution Hardening Effect of Ir" 479: 703–6. https://doi.org/10.4028/www.scientific.net/MSF.475-479.703.

Yamamoto, Takafumi, Masanori Hara, and Yuji Hatano. 2021. "Cracking Behavior and Microstructural, Mechanical and Thermal Characteristics of Tungsten–Rhenium Binary Alloys Fabricated by Laser Powder Bed Fusion." *International Journal of Refractory Metals and Hard Materials* 100 (November): 105651. https://doi.org/10.1016/J.IJRMHM.2021.105651.

Yar, M. A., Sverker Wahlberg, Hans Bergqvist, H. G. Salem, Mats Johnsson, and Mamoun Muhammed. 2011. "Spark Plasma Sintering of Tungsten-Yttrium Oxide Composites from Chemically Synthesized Nanopowders and Microstructural Characterization." *Journal of Nuclear Materials* 412 (2). https://doi.org/10.1016/j.jnucmat.2011.03.007.

Yin, Chao, Dmitry Terentyev, Tao Zhang, Shuhei Nogami, Steffen Antusch, Chih Cheng Chang, Roumen H. Petrov, and Thomas Pardoen. 2021. "Ductile to Brittle Transition Temperature of Advanced Tungsten Alloys for Nuclear Fusion Applications Deduced by Miniaturized Three-Point Bending Tests." *International Journal of Refractory Metals and Hard Materials* 95. https://doi.org/10.1016/j.ijrmhm.2020.105464.

Yin, Chao, Dmitry Terentyev, Tao Zhang, Roumen H. Petrov, and Thomas Pardoen. 2020. "Impact of Neutron Irradiation on the Strength and Ductility of Pure and ZrC Reinforced Tungsten Grades." *Journal of Nuclear Materials* 537. https://doi.org/10.1016/j.jnucmat.2020.152226.

Yoshiyasu ITOH** and Yutaka ISHIWATA**. 1996. "Strength Properties of Yttrim-Oxide-Dispersed Tungsten Alloy." *JSME International* 39: 429–34.

Zhang, Yue, Artur V. Ganeev, Jing Tao Wang, Jin Qiang Liu, and Igor V. Alexandrov. 2009. "Observations on the Ductile-to-Brittle Transition in Ultrafine-Grained Tungsten of Commercial Purity." *Materials Science and Engineering: A* 503 (1–2). https://doi.org/10.1016/j.msea.2008.07.074.

Zhao, Mingyue, Zhangjian Zhou, Qingming Ding, Ming Zhong, and Kameel Arshad. 2015. "Effect of Rare Earth Elements on the Consolidation Behavior and Microstructure of Tungsten Alloys." *International Journal of Refractory Metals and Hard Materials* 48: 19–23. https://doi.org/10.1016/j.ijrmhm.2014.07.014.

Zhao, Siqi, Yongqi Lv, Ziwei Zhang, and Jinglian Fan. 2024. "Synthesis and Characterization of W-Y2O3 Composites with Core-Shell Structure via Wet Chemical Method in an Acidic Solution." *International Journal of Refractory Metals and Hard Materials* 122 (August): 106729. https://doi.org/10.1016/J.IJRMHM.2024.106729.

Zhou, Zhangjian, Jun Tan, Dandan Qu, Gerald Pintsuk, Manfred Rödig, and Jochen Linke. 2012. "Basic Characterization of Oxide Dispersion Strengthened Fine-Grained Tungsten Based Materials Fabricated by Mechanical Alloying and Spark Plasma Sintering." *Journal of Nuclear Materials* 431 (1–3). https://doi.org/10.1016/j.jnucmat.2011.11.039.